International Journal of Mathematical, Engineering and Management Sciences
Vol. 8, No. 4, 787-803, 2023
https://doi.org/10.33889/IJMEMS.2023.8.4.045

Non-dyadic Haar Wavelet Algorithm for the Approximated Solution of Higher order Integro-Differential Equations

Ratesh Kumar
Department of Mathematics,
Lovely Professional University, Phagwara, 144411, Punjab, India.
E-mail: rateshqadian@gmail.com, ratesh.11755@lpu.co.in

Sabiha Bakhtawar
Department of Mathematics,
Lovely Professional University, Phagwara, 144411, Punjab, India.
Corresponding author: sabihabakhtawar1997@gmail.com, sabiha.12015214@lpu.in

(Received on January 10, 2023; Accepted on April 12, 2023)

Abstract
The objective of this study is to explore non-dyadic Haar wavelets for higher order integro-differential equations. In this research article, non-dyadic collocation method is introduced by using Haar wavelet for approximating the solution of higher order integrodifferential equations of Volterra and Fredholm type. The highest order derivatives in the integrodifferential equations are approximated by the finite series of non-dyadic Haar wavelet and then lower order derivatives are calculated by the process of integration. The integro-differential equations are reduced to a set of linear algebraic equations using the collocation approach. The Gauss - Jordan method is then used to solve the resulting system of equations. To demonstrate the efficiency and accuracy of the proposed method, numerous illustrative examples are given. Also, the approximated solution produced by the proposed wavelet technique have been compared with those of other approaches. The exact solution is also compared to the approximated solution and presented through tables and graphs. For various numbers of collocation points, different errors are calculated. The outcomes demonstrate the effectiveness of the Haar approach in resolving these equations.

Keywords- Fredholm integro-differential equations, Volterra integro-differential equations, Non-dyadic Haar wavelets, Collocation method.

1. Introduction

The solutions of differential and integro-differential equations (IDES) have become highly significant across several fields of science and engineering during the past few years. Many of the researchers are working to handle the different kinds of complexities while formulating the mathematical models (Yan et al., 2023), (Gao et al., 2023) to study the real time phenomenon. Many problems appearing in science and engineering of real-life phenomena are modelled by using IDES. The IDES find their applications in chemical kinetics, fluid dynamics, aerospace system, potential theory etc (Khan et al., 2022). A variety of differential equations having initial and boundary constraints arising in science and engineering presenting significant phenomenon can be transformed into integrodifferential equations. More specifically, IDEs can be used to create models that explain hereditary properties. These equations are difficult to solve analytically and require time-consuming calculations. As a result, most of the researchers presented computational methods for addressing such types of equations.

In recent years, the approximation theory for functional equations has gained a lot of interest, and several researchers have proposed numerical techniques for solving these equations. There are a variety of analytical and numerical methods to solve integro-differential (ID) equations including Taylor collocation method (Yalcinbas and Sezer, 2000), Adomain decomposition method (Wazwaz, 2001), Tau method

(Hosseini and shahmorad, 2003), Chebyshev collocation method (Akyüz and Sezer, 2005), Rational Haar function method (Maleknejad and Mirzaee, 2006), Sine-cosine wavelet method (Kajani et al., 2006), Finite difference method (Zhao and Coreless, 2006), Differential transform method (Darania and Ebadian, 2007), Homotopy pertibution method (Yusufoğlu, 2009), Bessel polynomial method (Yüzbaşı et al., 2011), Monotone iterative method (Al-Mdallal, 2012), Meshless method (Dehghan and Salehi, 2012), Improved Haar wavelet collocation method (Aziz and Al-Fhaid, 2014), Legendre wavelet (Chandel et al., 2015), Multiscale galerkin method (Chen et al., 2015), Sectorial operators (Raja et al., 2022), Shifted legendre polynomial is used for approximating the solution of ID difference equations (Saadatmandi and Dehghan, 2010). The primary objective of the study is to use Legendre polynomials as a method of finding a solution to ID-difference equation of higher order. To solve these equations analytically is generally getting more difficult. Expanding the approximate solution in terms of shifted Legendre polynomials having unknown coefficients, the problem has been reduced to a set of linear equations. Then, the value of coefficients of Legendre polynomials are determined by using the tau method and the operational matrices of delay and derivative. The authors provide illustrative numerical examples and a comparison to prior research to prove the effectiveness of the proposed technique. The singular higher order integro-differential equations have been solved analytically by using B-spline collocation method (Zemlyanova and Machina, 2020). Using the B-spline method, author introduce two computational schemes for approximating the solution to systems of integro-differential equations that arise in Steigmann-Ogden surface energy crack problems. The corresponding linear systems have been demonstrated to be well-conditioned, and numerical experiments agree well with their standard solutions. The author claims that even though this article focuses on a specific singular equation, the proposed method can easily be applied to more such type of problems. The Haar wavelet has been applied for obtaining the solution of integro-differential equations of third order (Alqarni et al., 2021). The author uses the Haar collocation algorithm to provide a numerical solution to IDE of 3rd order subject to boundary constraints. The technique is applicable to the solution of both linear as well as nonlinear IDES. In both nonlinear as well as linear integro-differential equations, Haar functions are used to approximatively represent the third-order derivative. Values of lower order derivative and the solution to the unknown function can be obtained via integration process. For solving linear systems, the Gauss elimination technique has been used, while for nonlinear systems, the Broyden technique is favoured. Several examples serve to demonstrate the validity and convergence of the presented algorithm. Also, the existence and uniqueness of solution of IDES of 3^{rd} order having initial conditions via Haar wavelet has been proved (Amin et al., 2023). Wavelets are contemporary orthonormal functions that can dilate and translate. Such characteristic makes wavelet based numerical methods qualitatively better than other methods. In literature, dyadic wavelets play a large role. Chui and Lian created non-dyadic Haar wavelets utilising multiresolution analysis (Chui and Lian, 1995). The non-dyadic Haar wavelets are used in the literature for solving various differential model, such as Boundary value problems (Arora at al., 2018) Fractional - Burgers' equation (Arora et al., 2020), and Fisher Kolmogorov Petrovsky equation (Kumar and Arora, 2022) etc.

However, non-dyadic Haar wavelets have not yet been utilized to solve higher order integro-differential equations, which is the primary motivation for solving higher order integro-differential equations. In this manuscript, we have approximated the solution of higher-order integrodifferential equations by utilizing nondyadic Haar wavelets. The rest of manuscript is structured as, the basic preliminaries related to non-dyadic Haar wavelets is presented in section 2 of the manuscript. The main algorithm that is constructed by using non-dyadic Haar wavelets is presented in section 3. In order to check the validation of the presented algorithm, some experiments have been performed that are explained in section 4. The whole manuscript is concluded in section 5.

2. Non-Dyadic Haar Wavelets

In a dyadic Haar wavelet, the whole wavelet family is generated by only one mother wavelet, whereas in non-dyadic Haar wavelet, the wavelet family is generated by two mother wavelets having different shapes and different characteristics. Standard representation of non-dyadic Haar wavelet is presented here (Chui and Lian, 1995; Mittal and Pandit, 2017).

Haar scaling function

$$\psi_1(z) = \phi^0(z) = \begin{cases} 1 & z \epsilon\, [0,1] \\ 0 & otherwise \end{cases} \tag{1}$$

Symmetric Haar wavelet

$$\psi_i(z) = \phi^1(3^j z - k) = \frac{1}{\sqrt{2}} \begin{cases} -1 & z \epsilon \left[\gamma_1(i),\ \gamma_2(i)\right) \\ \ \ 2 & z \epsilon \left[\gamma_2(i),\ \gamma_3(i)\right) \\ -1 & z \epsilon \left[\gamma_3(i),\ \gamma_4(i)\right) \\ \ \ 0 & otherwise \end{cases} \quad for\ i = 2, 4, \dots, 3p-1 \tag{2}$$

Anti-Symmetric Haar wavelet

$$\psi_i(z) = \phi^2(3^j z - k) = \sqrt{\frac{3}{2}} \begin{cases} \ \ 1 & z \epsilon \left[\gamma_1(i),\ \gamma_2(i)\right) \\ \ \ 0 & z \epsilon \left[\gamma_2(i),\ \gamma_3(i)\right) \\ -1 & z \epsilon \left[\gamma_3(i),\ \gamma_4(i)\right) \\ \ \ 0 & otherwise \end{cases} \quad for\ i = 3, 6, \dots, 3p \tag{3}$$

where,

$$\gamma_1(i) = \frac{k}{p}, \gamma_2(i) = \frac{3k+1}{3p},\ \gamma_3(i) = \frac{3k+2}{3p}, \gamma_4(i) = \frac{k+1}{p}, p = 3^j,$$
$$j = 0, 1, 2, \dots\ and\ \ k = 0, 1, 2, \dots p-1.$$

Here i is the wavelet number, dilation factor is represented by the variable j, and the translation parameter is represented by k for the wavelet family. The values of i can be easily computed from the expression $i - 1 = 3^j + 2k$ (for those wavelet numbers i that are multiples of 2) and $i - 2 = 3^j + 2k$ (for other remaining wavelet numbers i).

Eq.(1) − Eq. (3) can be integrated easily over the interval [A, B) the required number of times, by using the formula which is given as

$$q_{\delta,i}(z) = \frac{1}{\Gamma(\delta)} \int_A^z \psi_i(x)(z-x)^{\delta-1} dx; \delta \epsilon\, [0, m], m = 1, 2, 3, \dots \quad and\ i = 1, 2, 3, \dots 3p \tag{4}$$

After calculating the above integrals, the value of integrals is:

$$q_{\delta,i}(z) = \frac{z^\delta}{\Gamma(\delta+1)} \quad , \quad for\ i = 1 \tag{5}$$

$q_{\delta,i}(z)'s\ \ for\ \ i = 2,4,6,8, \cdots, 3p-1$ are given by

$$q_{\delta,i}(z) = \sqrt{\frac{1}{2}}\begin{cases} 0 & z \in [0,\ \gamma_1(i)) \\ \frac{-1}{\Gamma(\delta+1)}(z-\gamma_1(i))^{\delta} & z \in [\gamma_1(i),\ \gamma_2(i)) \\ \frac{1}{\Gamma(\delta+1)}\left[-\left(z-\gamma_1(i)\right)^{\delta} + 3\left(z-\gamma_2(i)\right)^{\delta}\right] & z \in [\gamma_2(i),\ \gamma_3(i)) \\ \frac{1}{\Gamma(\delta+1)}\left[-\left(z-\gamma_1(i)\right)^{\delta} + 3\left(z-\gamma_2(i)\right)^{\delta} - 3\left(z-\gamma_3(i)\right)^{\delta}\right] & z \in [\gamma_3(i),\ \gamma_4(i)) \\ \frac{1}{\Gamma(\delta+1)}\left[-\left(z-\gamma_1(i)\right)^{\delta} + 3\left(z-\gamma_2(i)\right)^{\delta} - 3\left(z-\gamma_3(i)\right)^{\delta} + \left(z-\gamma_4(i)\right)^{\delta}\right] & z \in [\gamma_4(i), 1) \end{cases} \tag{6}$$

$q_{\delta,i}(z)'s \ \ for \ \ i = 3,5,7,9,\cdots,3p$ are given by

$$q_{\delta,i}(z) = \sqrt{\frac{3}{2}}\begin{cases} 0 & z \in [0,\ \gamma_1(i)) \\ \frac{1}{\Gamma(\delta+1)}(z-\gamma_1(i))^{\delta} & z \in [\gamma_1(i),\ \gamma_2(i)) \\ \frac{1}{\Gamma(\delta+1)}\left[\left(z-\gamma_1(i)\right)^{\delta} - \left(z-\gamma_2(i)\right)^{\delta}\right] & z \in [\gamma_2(i),\ \gamma_3(i)) \\ \frac{1}{\Gamma(\delta+1)}\left[\left(z-\gamma_1(i)\right)^{\delta} - \left(z-\gamma_2(i)\right)^{\delta} - \left(z-\gamma_3(i)\right)^{\delta}\right] & z \in [\gamma_3(i), \gamma_4(i)) \\ \frac{1}{\Gamma(\delta+1)}\left[\left(z-\gamma_1(i)\right)^{\delta} - \left(z-\gamma_2(i)\right)^{\delta} - \left(z-\gamma_3(i)\right)^{\delta} + \left(z-\gamma_4(i)\right)^{\delta}\right] & z \in [\gamma_4(i), 1) \end{cases} \tag{7}$$

In Haar scale 3 wavelet collocation approach, collocation point for the interval $[A, B]$ is given by the relation

$$z_m = A + (B-A)\frac{m-0.5}{3p};\ m = 1, 2, 3, \ldots, 3p \tag{8}$$

3. Non-Dyadic Haar Wavelet Collocation Algorithm (NDHWCA)

In this section, a numerical method has been designed by utilizing non-dyadic Haar wavelets for approximating the solutions of higher order integrodifferential equations.

3.1 Lemma 1

If $u(z) \in l^2(R)$ over the interval $[A, B]$ such that $u(z) = \sum_{i=0}^{3p} a_i\psi_i(z)$ then the value of integral in (Aziz and Haq, 2010; Kumar and Bakhtawar, 2022) is given by

$$\int_A^B u(z)\,dz = \frac{B-A}{3p}\sum_{m=1}^{3p} u(z_m) = \frac{B-A}{3p}\sum_{m=1}^{3p} u\left(A + (B-A)\left(\frac{m-0.5}{3p}\right)\right) \tag{9}$$

3.2 Method of Solution

Now consider n^{th} order integrodifferential equations

$$u^{(n)}(z) + m(z)u^{(n-1)}(z) + \cdots + n(z)u(z) = \mu_1\int_m^n w_1(z,y)u(y)dy + \mu_2\int_m^z w_2(z,y)u(y)dy + g(z) \tag{10}$$

With initial conditions $u(0) = \theta_1, u'(0) = \theta_2, u''(0) = \theta_3, \ldots. u^{(n-1)}(0) = \theta_n$.

Here m and n are functions of z. w_1 and w_2 are kernels or nucleus of integration. $\mu_1, \mu_2, \theta_1, \theta_2, \ldots, \theta_n$ are real constants. $g(z)$ is known function which is already given. The primary objective is to find the value of unknown function $u(z)$ that will satisfy the integrodifferential Eq. (10).

Now assume that

$$u^{(n)}(z) = \sum_{i=1}^{3p} a_i \psi_i(z) \tag{11}$$

Integrating Eq. (11) from 0 to z and by using initial conditions

$$u^{(n-1)}(z) - u^{(n-1)}(0) = \sum_{i=1}^{3p} a_i L_{i,1}(z) \;;\; where\ L_{i,\ 1}(z) = \int_0^z \psi_i(z)\, dz \tag{12}$$

$$u^{(n-1)}(z) = \theta_n + \sum_{i=1}^{3p} a_i L_{i,1}(z) \;;\; where\ L_{i,\ 1}(z) = \int_0^z \psi_i(z)\, dz \tag{13}$$

Again, integrating Equation (13) and by using the initial conditions value of $u^{(n-2)}(z)$ will be obtained. By doing the same procedure, values of all lower order derivatives $u^{(n-3)}(z)$, $u^{(n-4)}(z)$, $u^{(n-5)}(z)$,… and for the unknown function $u(z)$ would be obtained. By substituting all the values in integrodifferential equations and the integrals involved are calculated by the formula given in Equation (9) and by putting the collocation points a $3p \times 3p$ system of equations is obtained. This system of equations is then solved by using the Gauss elimination method (GEM) for finding the values of unknown Haar coefficients. Finally, by putting these coefficients solution at collocations points has been obtained.

4. Numerical Experiments

For checking the accuracy of the method, the method is implemented to different experiments and the results obtained by this method are compared with results already available in the literature. The maximum absolute error, $l_2 - error,\ E_{max} - error, and\ l_\infty - error$ has been calculated for checking the accuracy of the presented algorithm, by using the MATLAB software, where u_{ap} is the approximate solution (AE) and u_{ex} is the exact solution (ES) at different collocation points. The relation for calculating E_{cp} and M_{cp} (Amin et al., 2023).

$$l_2 - error = \frac{\sqrt{\sum_{i=1}^{3p} \left|u(z_m)_{ex} - u(z_m)_{ap}\right|^2}}{\sum_{i=1}^{3p} |u(z_m)_{ex}|^2}, E_{max} - error = \sqrt{\sum_{i=1}^{3p} \left|u(z_m)_{ex} - u(z_m)_{ap}\right|^2}.$$

$$l_\infty - error = E_{cp} = max\left|u(z_m)_{ex} - u(z_m)_{ap}\right|, M_{cp} = \sqrt{\frac{\sum_{i=1}^{3p} \left|u(z_m)_{ex} - u(z_m)_{ap}\right|^2}{3p}}.$$

$$Absolute - error = \left|u(z_m)_{ex} - u(z_m)_{ap}\right|.$$

***Experiment* 1:** Consider the 1st order Volterra IDES (Wazwaz, 2011).

$$u'(z) = 1 - 2\, z\, sin(z) + \int_0^z u(t)dt \quad ; u(0) = 0 \tag{14}$$

The ES found from the literature is $u(z) = z \cos(z)$ and the solution obtained by using the presented technique is $u(z) = \sum_{i=1}^{3p} a_i L_{i,1}(z)$.

Table 1. Computation of exact and approximated solution for experiment 1.

z	ES	AS	Value of Absolute Error
0.05555556	0.05546984	0.05529813	1.72E-04
0.16666667	0.16435721	0.16384454	5.13E-04
0.27777778	0.26712977	0.26628349	8.46E-04
0.38888889	0.35985091	0.35868307	1.17E-03
0.50000000	0.43879128	0.43731840	1.47E-03
0.61111111	0.50050672	0.49874944	1.76E-03
0.72222222	0.54191119	0.53989379	2.02E-03
0.83333333	0.56034354	0.55809342	2.25E-03
0.94444444	0.55362678	0.55117387	2.45E-03

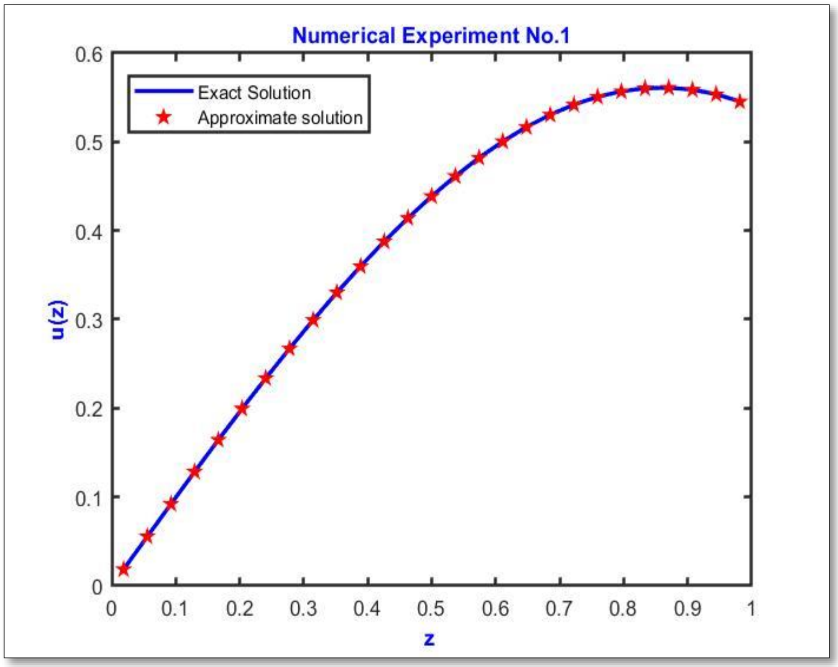

Figure 1. Graphical comparison of ES and AS for Experiment 1.

The solution obtained by the proposed method is compared with that of ES, which is presented in Table 1 and Figure 1. $l_2 - error$, $l_\infty - error$, and $E_{max} - error$ for different values of j are calculated and is presented in Table 2. From Table 2, it can be observed that by increasing the values of j error decreases. The obtained result is compared with already existing results in the literature. The error obtained by using the presented algorithm for $j = 2$ is 10^{-4} whereas by using Haar wavelet and Legendre wavelet the error is 10^{-2} and 10^{-3} respectively as shown in Table 2. From Figure 1, it can be observed that the approximated solution coincides well with that of exact solution, which proves the convergence of the proposed method. Figure 2 represents the absolute value of error for different collocation points. The better accuracy of the results can be achieved by increasing the level of resolution j.

Table 2. Computation of errors for Experiment 1.

j	$l_2 - error$	$l_\infty - error$	$E_{max} - error$	$E_{max} - error$ by using Haar method (Shiralashetti, 2017)	$E_{max} - error$ by using Legendre method (Shiralashetti, 2017)
0	3.43E-02	2.06E-02	2.51E-02	----------	---------
1	3.79E-03	2.45E-03	4.77E-03	----------	---------
2	4.20E-04	2.79E-04	9.17E-04	1.37e-02	1.21e-03
3	4.67E-05	3.12E-05	1.77E-04	3.49e-03	3.10e-04
4	5.19E-06	3.47E-06	3.40E-05	8.81e-04	7.82e-05
5	5.77E-07	3.86E-07	6.54E-06	2.20e-04	1.96e-05

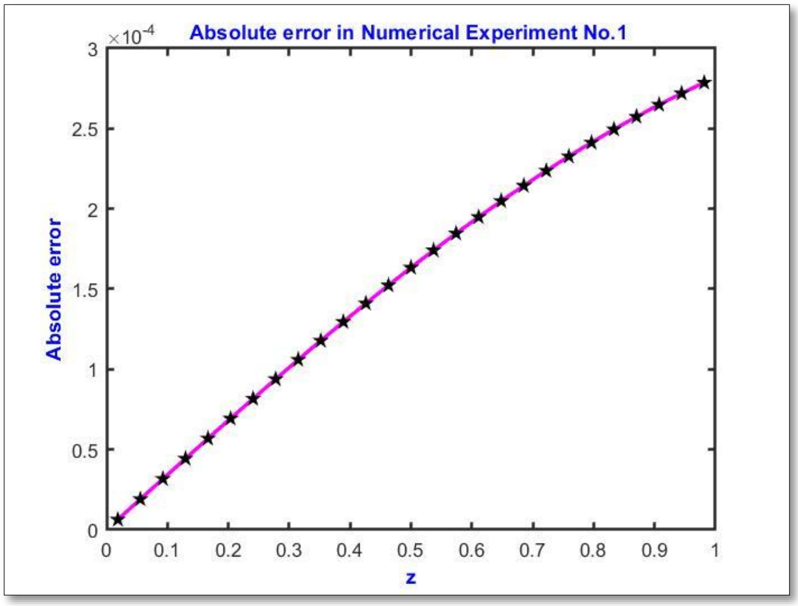

Figure 2. Graph of absolute error for Experiment 1.

***Experiment* 2:** Consider the 2nd order Fredholm IDE (Rahman, 2007).

$$u''(z) = e^z - z + z\int_0^1 t\, u(t)dt \quad ; u(0) = 1\,, u'(0) = 1 \tag{15}$$

The ES obtained from literature is $u(z) = e^z$ whereas the AS obtained by using the proposed method is $u(z) = 1 + z + \sum_{i=1}^{3p} a_i L_{i,2}(z)$.

Table 3. Computation of exact and approximated solution for experiment 2.

z	ES	AS	Value of Absolute Error
0.055555556	1.057127745	1.057127677	6.74E-08
0.166666667	1.181360413	1.181358593	1.82E-06
0.277777778	1.320192788	1.320184363	8.43E-06
0.388888889	1.475340615	1.475317497	2.31E-05
0.500000000	1.648721271	1.648672135	4.91E-05
0.611111111	1.842477459	1.842387747	8.97E-05
0.722222222	2.059003694	2.058855612	1.48E-04
0.833333333	2.300975891	2.300748409	2.27E-04
0.944444444	2.571384435	2.571053288	3.31E-04

The solution obtained by the proposed method is compared with that of ES and presented in Table 3 and Figure 3 for Experiment 2. The $l_2 - error,\ l_\infty - error, and\ E_{max} - error$ are calculated for different values of j for Experiment 2 which is presented in Table 4. The value of absolute error is presented graphically in Figure 4. From Table 4, it can be observed that by increasing the value of j error decreases. The results obtained are compared with the results calculated by using Haar wavelets and cosine and sine wavelet methods in the literature. The error obtained by using the proposed method for $j = 5$ is 10^{-7} where as the error is 10^{-5} and 10^{-6} in case of Haar wavelet method and Cosine Sine wavelet method respectively as presented in Table 4. Figure 3 shows that the estimated solution closely matches the precise solution, demonstrating the convergence of the proposed approach. An improved level of precision in the results can be attained by increasing the resolution j.

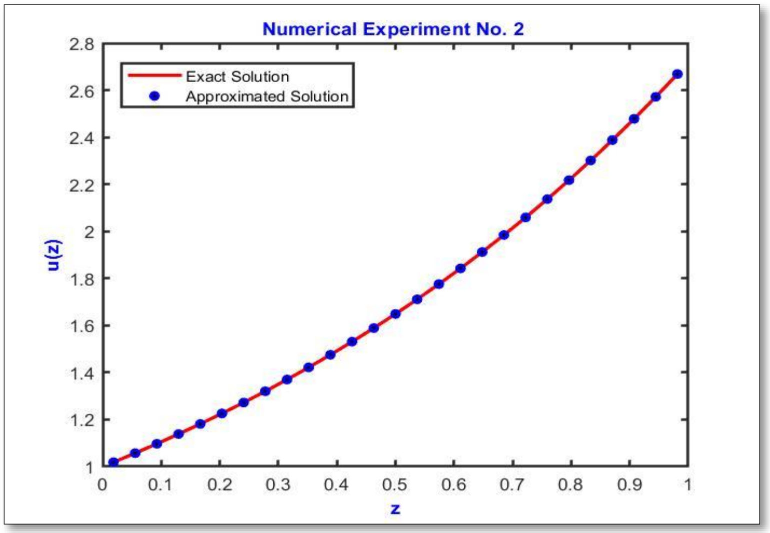

Figure 3. Graphical comparison of ES and AS for experiment 2.

Table 4. Computation of errors for experiment 2.

j	$l_2 - error$	$l_\infty - error$	$E_{max} - error$	$E_{max} - error$ (Shiralashetti, 2017)	$E_{max} - error$ (Shiralashetti, 2017)
0	6.78E-04	2.03E-03	2.07E-03	-------	-------
1	8.23E-05	3.31E-04	4.41E-04	-------	-------
2	9.23E-06	4.13E-05	8.58E-05	3.07e-03	4.09e-04
3	1.03E-06	4.77E-06	1.65E-05	8.48e-04	1.13e-04
4	1.14E-07	5.36E-07	3.18E-06	2.22e-04	2.96e-04
5	1.27E-08	5.98E-08	6.12E-07	5.69e-05	7.60e-06

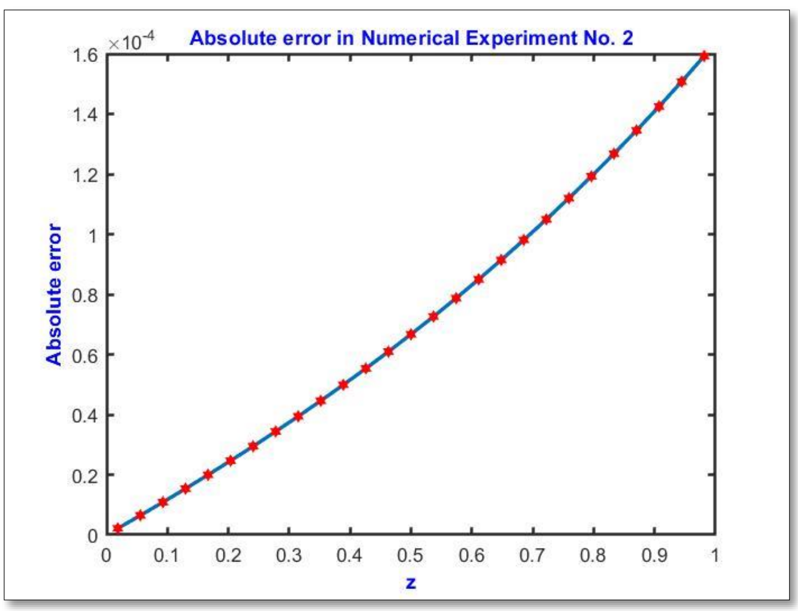

Figure 4. Graph of absolute error for experiment 2.

Experiment* 3*: Consider the 8th order IDE of Fredholm type (Shang and Han, 2010).

$$u^8(z) = -8e^z + z^2 + u(z) + \int_0^1 z^2\, u'(t)dt \tag{16}$$

with initial conditions $u(0) = 1, u'(0) = 0, u''(0) = -1$ $u'''(0) = -2, u^{(4)}(0) = -3, u^{(5)}(0) = -4, u^{(6)}(0) = -5, u^{(7)}(0) = -6$.

The ES for obtained from literature is $u(z) = (1 - z)e^z$ and the AS is $u(z) = 1 - \frac{z^2}{2} - \frac{z^3}{3} - \frac{z^4}{8} - \frac{z^5}{30} - \frac{z^6}{144} - \frac{z^7}{840} + \sum_{i=1}^{3p} a_i L_{i,8}(z)$.

Table 5. Computation of exact and approximated solution for experiment 3.

z	ES	AS	Value of Absolute Error
0.055555556	0.998398426	0.998398426	1.11E-14
0.166666667	0.984467011	0.984467011	4.50E-12
0.277777778	0.953472569	0.953472569	1.91E-10
0.388888889	0.901597043	0.901597041	2.10E-09
0.500000000	0.824360635	0.824360623	1.23E-08
0.611111111	0.716519012	0.716518963	4.90E-08
0.722222222	0.571945471	0.571945319	1.52E-07
0.833333333	0.383495982	0.383495595	3.87E-07
0.944444444	0.142854691	0.142853848	8.43E-07

The solution obtained by the proposed method is compared with that of ES and is presented in Table 5 and Figure 5 for Experiment 3. The $l_2 - error$, $l_\infty - error$, and $E_{max} - error$ are calculated for different values of j for Experiment 3 which is presented in Table 6, and it can be observed that by increasing the values of j error decreases. The graph for absolute error for level of resolution 2 is presented in Figure 6. It is possible to deduce that the proposed technique converges on the exact solution based on the fact that the approximated solution closely matches that of the precise solution, as can be seen in Figure 5. The absolute value of the error across all the different collocation points is displayed in Figure 6. By raising the degree of resolution j, one can improve the precision of the outcomes obtained.

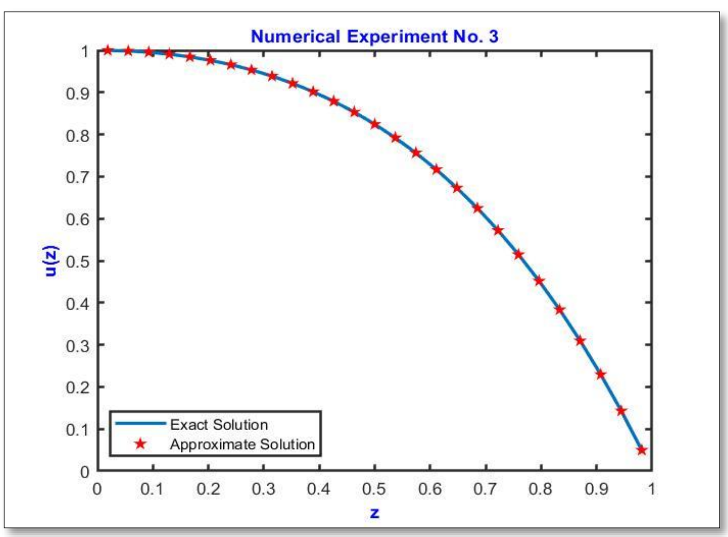

Figure 5. Graphical comparison of ES and AS for experiment 3.

Table 6. Computation of errors for experiment 3.

j	$l_2 - error$	$l_\infty - error$	$E_{max} - error$
0	2.94E-06	3.94E-06	3.95E-06
1	4.06E-07	8.43E-07	9.41E-07
2	9.13E-08	2.88E-07	3.67E-07

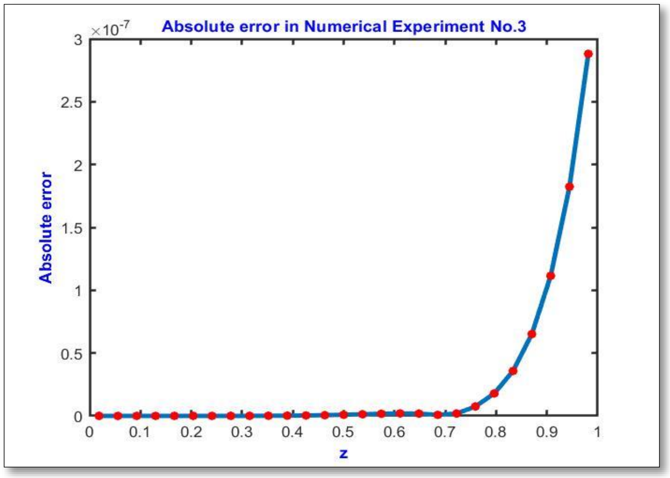

Figure 6. Graph of absolute error for experiment 3.

Experiment 4: Consider the Volterra IDE of 3rd order (Yüzbaşı et al., 2011).

$$u'''(z) - zu''(z) = \frac{4}{7}z^9 - \frac{8}{5}z^7 + 6z^2 - z^6 - 6 + 4\int_0^z z^2t^3u(t)dt \tag{17}$$

having initial conditions $u(0) = 1, u'(0) = 2$ and $u''(0) = 0$. The ES for this problem is $u(z) = 1 + 2z - z^3$ and the AS is $u(z) = 2z + \sum_{i=1}^{3p} a_i L_{i,3}(z) \ + 1$.

The computation of ES and AS for different collocation points (when level of resolution is 1) is presented in Table 7. The value of absolute error is also calculated and presented in Table 7. Different errors are calculated for different resolution level and presented in Table 8. In Table 8, a comparison is also made among the value of M_{cp} and E_{cp} errors with existing results in the literature (Amin et al., 2023) and it can be observed that our results are much better than the previous one. The graph for absolute error which is 10^{-16} is presented in Figure 8 for level of resolution 2. The graphical comparison of approximated and exact solution for different collocation points is displayed in Figure 7, and it can be observed that the graph exactly coincides on one another proving the convergence of the method.

Table 7. Computation of exact and approximated solution for experiment 4.

z	ES	AS	Value of Absolute Error
0.055555556	1.110939643	1.110939643	0
0.166666667	1.328703704	1.328703704	0
0.277777778	1.534122085	1.534122085	0
0.388888889	1.718964335	1.718964335	0
0.500000000	1.875000000	1.875000000	0
0.611111111	1.993998628	1.993998628	2.22045E-16
0.722222222	2.067729767	2.067729767	0
0.833333333	2.087962963	2.087962963	0
0.944444444	2.046467764	2.046467764	0

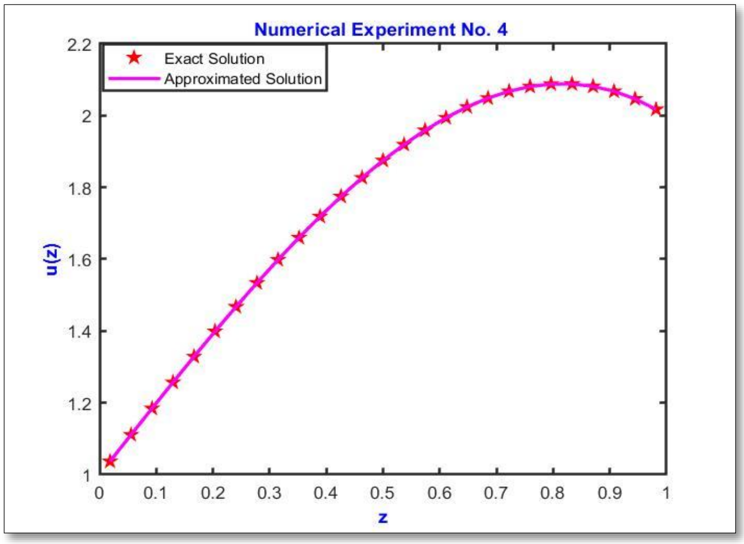

Figure 7. Graphical comparison of ES and AS for experiment 4.

Table 8. Computation of errors for experiment 4.

j	$l_2 - error$	$E_{max} - error$	$M_{cp} - error$	$M_{cp} - error$ (Amin et al., 2023)	$E_{cp} - error$	$E_{cp} - error$ (Amin et al., 2023)
0	0	0	0	2.68E-05	0	5.36E-05
1	4.15E-17	2.22E-16	7.40E-17	7.65E-06	2.22E-16	2.08E-05
2	8.31E-17	7.69E-16	1.48E-16	1.98E-06	4.44E-16	6.70E-06
3	5.18E-17	8.31E-16	9.23E-17	5.01E-07	4.44E-16	1.91E-06
4	4.80E-17	1.33E-15	8.55E-17	1.25E-07	4.44E-16	5.12E-07
5	3.03E-17	1.46E-15	5.39E-17	3.14E-08	4.44E-16	1.32E-07

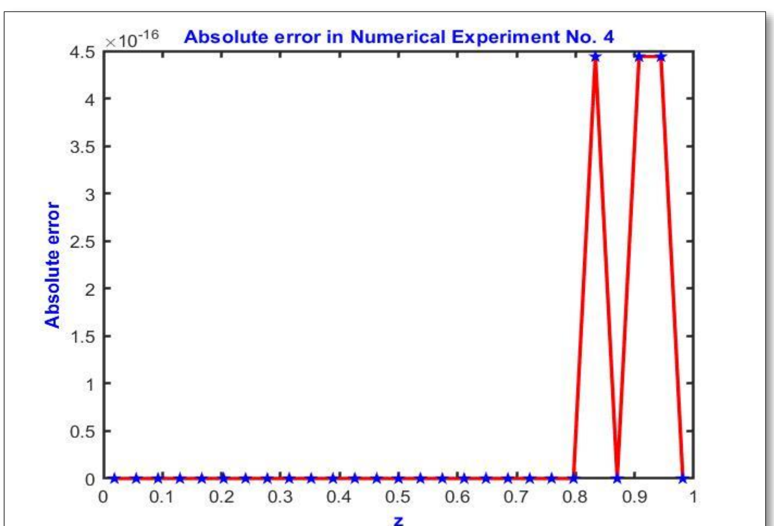

Figure 8. Graph of absolute error for experiment 4.

***Experiment* 5:** Consider the Fredholm IDE of 3rd order (Gegele et al., 2014).

$$u'''(z) = 1 - e + e^z + \int_0^1 u(t)dt \tag{18}$$

having initial conditions $u(0) = u'(0) = u''(0) = 1$.

The ES for this Fredholm equation is $u(z) = e^z$ and the AS is $u(z) = z + \frac{z^2}{2} + \sum_{i=1}^{3p} a_i L_{i,3}(z) + 1$.

The computation of ES and AS for different collocation points (when level of resolution is 1) is presented in Table 9. The value of absolute error is also calculated and presented in Table 9. Different errors are calculated for various resolution level and presented in Table 10. In Table 10, a comparison is presented for different value of M_{cp} and E_{cp} errors with existing results in the literature (Amin et al., 2023). The graph for absolute error which is 10^{-5} is presented in Figure 10 for level of resolution 2. Figure 9 shows a graphic comparison between the approximated and exact solutions for several collocation points, making it obvious that the graphs precisely overlap on one another, demonstrating the method's convergence.

Table 9. Computation of exact and approximated solution for experiment 5.

z	ES	AS	Value of Absolute Error
0.055555556	1.057127745	1.057128982	1.23713E-06
0.166666667	1.181360413	1.181374950	1.45375E-05
0.277777778	1.320192788	1.320234909	4.21202E-05
0.388888889	1.475340615	1.475425767	8.51512E-05
0.500000000	1.648721271	1.648866171	1.44900E-04
0.611111111	1.842477459	1.842700212	2.22752E-04
0.722222222	2.059003694	2.059323918	3.20223E-04
0.833333333	2.300975891	2.301414864	4.38973E-04
0.944444444	2.571384435	2.571965258	5.80823E-04

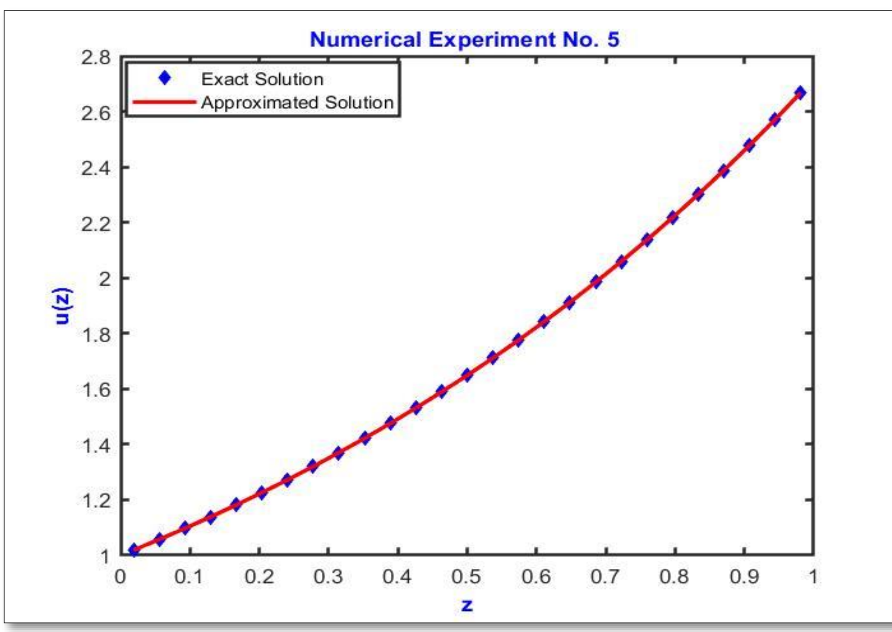

Figure 9. Graphical comparison of ES and AS for experiment 5.

Table 10. Computation of errors for experiment 5.

j	$l_2 - error$	$E_{max} - error$	$M_{cp} - error$	$M_{cp} - error$ (Amin et. al., 2023)	$E_{cp} - error$	$E_{cp} - error$ (Amin et. al., 2023)
0	1.35E-03	4.14E-03	2.39E-03	1.10E-03	3.94E-03	1.95E-03
1	1.58E-04	8.44E-04	2.81E-04	2.83E-04	5.81E-04	5.62E-04
2	1.76E-05	1.63E-04	3.15E-05	7.13E-05	7.04E-05	1.50E-04
3	1.96E-06	3.15E-05	3.50E-06	1.78E-05	8.05E-06	3.88E-05
4	2.17E-07	6.06E-06	3.89E-07	4.46E-06	9.03E-07	9.87E-06
5	2.42E-08	1.17E-06	4.32E-08	1.11E-06	1.01E-07	2.48E-06

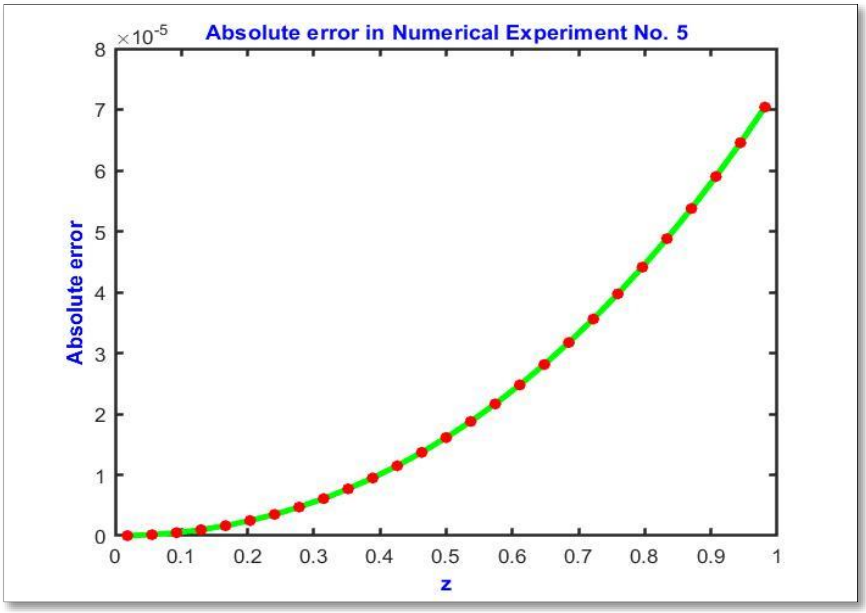

Figure 10. Graph of absolute error for experiment 5.

***Experiment* 6:** Consider the Fredholm IDE of 4^{th} order (Gegele et al., 2014).

$$u^{iv}(z) = \frac{1}{4} + (1 - 2ln2)z - \frac{6}{(1+z)^4} + \int_0^1 (z-t)u(t)dt \tag{19}$$

having initial conditions $u(0) = 0,\ u'(0) = 1,\ u''(0) = -1, u'''(0) = 2$. The ES obtained from literature is $u(z) = \ln(z+1)$ and the AS is $u(z) = z - \frac{z^2}{2} + \frac{z^3}{3} + \sum_{i=1}^{3p} a_i L_{i,4}(z)$.

The computation of ES and AS for different collocation points (when level of resolution is 4) is presented in Table 11. The value of absolute error is also calculated and presented in Table 11. A comparison is presented to the value of absolute error with that of power series method and Chebyshev series method (Gegele et al., 2014). Different errors are calculated for various resolution level and presented in Table 12. From Table 12, it can be observed that error becomes lesser as the value of j is raised. The graph for absolute error which is 10^{-4} is presented in Figure 12 for level of resolution 2. Figure 11 displays a graphical comparison of an approximated and an exact solution for several collocation points. It can be seen that the graphs perfectly coincide on one another, which proves that the technique successfully convergent.

Table 11. Computation of exact and approximated solution for experiment 6.

z	ES	AS	Value of Absolute Error	Value of Absolute Error by using Power series (Gegele et al., 2014)	Value of Absolute Error by using Chebyshev series (Gegele et al., 2014)
0.00	0.002055	0.002055	2.94E-14	0	2.70E-08
0.10	0.096058	0.096058	5.46E-09	6.01E-07	3.32E-07
0.20	0.185403	0.185403	4.27E-08	9.14E-06	4.23E-07
0.30	0.264262	0.264262	1.34E-07	6.21E-05	5.25E-06
0.40	0.337354	0.337354	3.02E-07	4.52E-05	2.37E-06
0.50	0.405465	0.405466	5.66E-07	3.36E-05	3.98E-05
0.60	0.471802	0.471803	9.64E-07	2.73E-05	2.17E-05
0.70	0.531596	0.531598	1.48E-06	1.64E-05	1.73E-05
0.80	0.588015	0.588017	2.15E-06	4.30E-04	1.27E-05
0.90	0.643585	0.643588	3.02E-06	2.01E-04	1.11E-05
0.99	0.692118	0.692122	4.00E-06	1.16E-04	3.17E-04

Table 12. Computation of errors for experiment 6.

j	$l_2 - error$	$E_{max} - error$	$M_{cp} - error$	$E_{cp} - error$
2	2.908011E-04	6.556580E-04	1.261814E-04	3.090407E-04
3	3.241298E-05	1.265906E-04	1.406562E-05	3.564459E-05
4	3.602701E-06	2.437114E-05	1.563410E-06	4.007867E-06

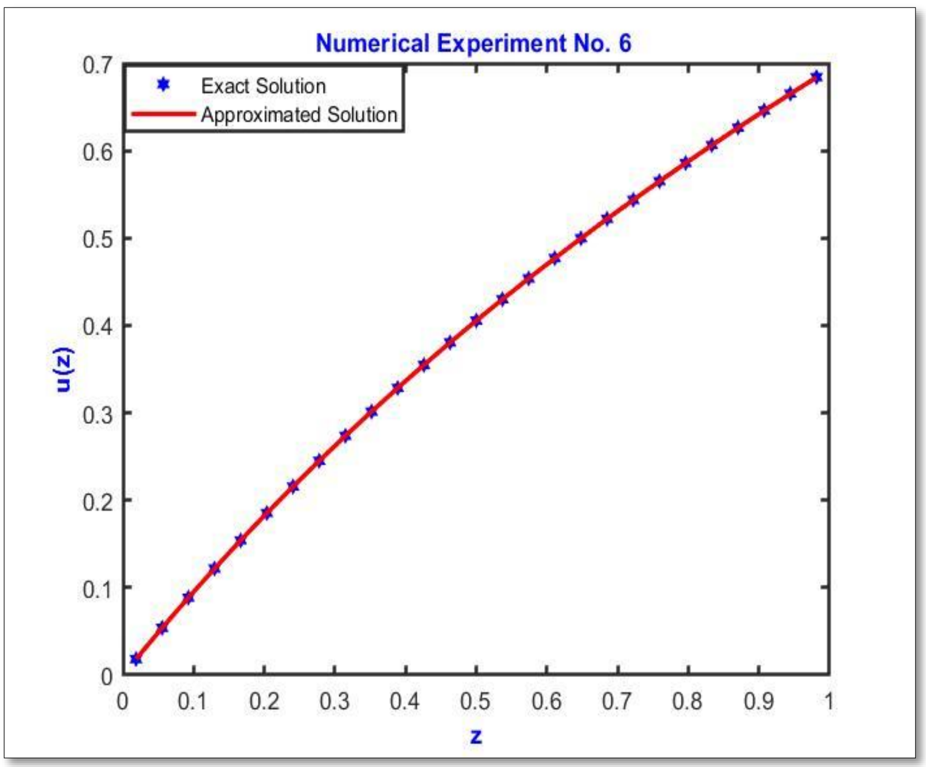

Figure 11. Graphical comparison of ES and AS for experiment 6.

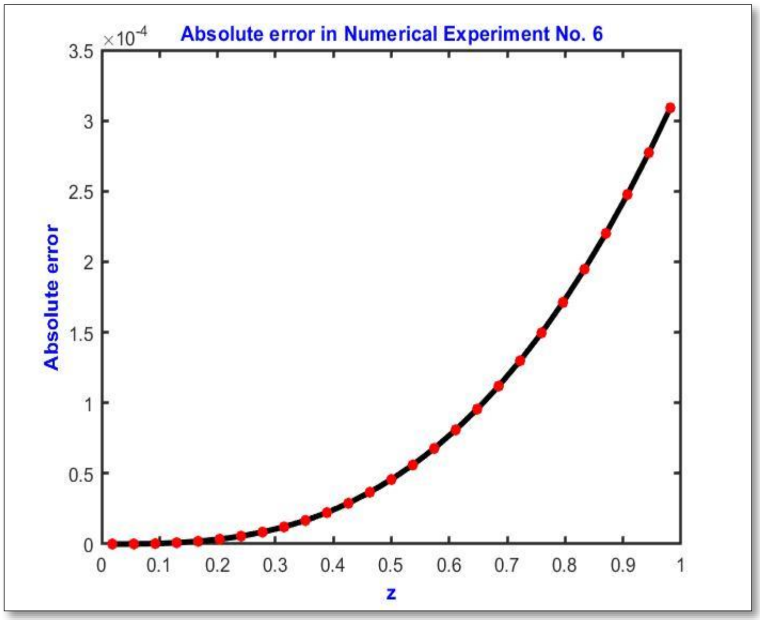

Figure 12. Graph of absolute error for experiment 6.

5. Conclusions and Future Scope

In this research article, Non-dyadic Haar wavelet collocation algorithm (NDHWCA) is presented for finding the approximate solution of Fredholm integrodifferential equations and Volterra integrodifferential equations of higher order. The highest order derivative is approximated by the non-dyadic Haar wavelets and then by using the process of integration lower order derivatives are obtained. The proposed method is applied to different experiments and the results obtained are much better than the previous results. Results is presented through tables and graphs. For all the computational work, MATLAB software is used. The following is an overview of the primary benefits of NDHWCA:

(i) The effectiveness and execution of NDHWCA with the use of MATLAB software can be easily achieved.
(ii) By increasing the dilation factor, error becomes lesser proving the convergence of the method.
(iii) The proposed algorithm converges faster than the Haar scale 2 wavelets.
(iv) As compared to other known methods, the NDHWCA has been shown to yield better results that are more accurate.
(v) The NDHWCA can be extended to resolve complex higher order integrodifferential equations having nonlinearity in them.
(vi) The proposed algorithm can also be extended for the solution of fractional integrodifferential equations.
(vii) The presented technique can also be extended to solve integral equations.

Conflict of Interest

The author(s) have no conflicts of interest.

Acknowledgements

The authors would like to thank the editor and anonymous reviewers for their valuable comments that help to improve the quality of this work. This work did not receive any financial funding.

References

Akyüz-Daşcıoğlu, A., & Sezer, M. (2005). Chebyshev polynomial solutions of systems of higher-order linear Fredholm–Volterra integro-differential equations. *Journal of the Franklin Institute*, *342*(6), 688-701.

Al-Mdallal, Q.M. (2012). Boundary value problems for nonlinear fractional integro-differential equations: theoretical and numerical results. *Advances in Difference Equations*, *2012*(1), 1-13.

Alqarni, M.M., Amin, R., Shah, K., Nazir, S., Awais, M., Alshehri, N.A., & Mahmoud, E.E. (2021). Solution of third order linear and nonlinear boundary value problems of integro-differential equations using Haar wavelet method. *Results in Physics*, *25*, 104176.

Amin, R., Shah, K., Awais, M., Mahariq, I., Nisar, K.S., & Sumelka, W. (2023). Existence and solution of third order integro-differential equations via Haar wavelet method. *Fractals*. https://doi.org/10.1142/S0218348X23400376.

Arora, G., Kumar, R., & Kaur, H. (2018). A novel wavelet based hybrid method for finding the solutions of higher order boundary value problems. *Ain Shams Engineering Journal*, *9*(4), 3015-3031.

Arora, G., Kumar, R., & Kaur, H. (2020). Scale-3 Haar wavelets and quasi linearization based hybrid technique for the solution of coupled space-time fractional-Burgers' equation. *Pertanika Journal of Science and Technology*, *28*(2), 579-607.

Aziz, I., & Al-Fhaid, A.S. (2014). An improved method based on Haar wavelets for numerical solution of nonlinear integral and integro-differential equations of first and higher orders. *Journal of Computational and Applied Mathematics*, *260*, 449-469.

Aziz, I., & Haq, F. (2010). A comparative study of numerical integration based on Haar wavelets and hybrid functions. *Computers & Mathematics with Applications*, *59*(6), 2026-2036.

Chandel, R.S., Singh, A., & Chouhan, D. (2015). Solution of higher order volterra integro-differential equations by Legendre wavelets. *International Journal of Applied Mathematics*, *28*(4), 377-390.

Chen, J., Huang, Y., Rong, H., Wu, T., & Zeng, T. (2015). A multiscale Galerkin method for second-order boundary value problems of Fredholm integro-differential equation. *Journal of Computational and Applied Mathematics*, *290*, 633-640.

Chui, C.K., & Lian, J.A. (1995). Construction of compactly supported symmetric and antisymmetric orthonormal wavelets with scale 3. *Applied and Computational Harmonic Analysis*, *2*(1), 21-51.

Darania, P., & Ebadian, A. (2007). A method for the numerical solution of the integro-differential equations. *Applied Mathematics and Computation*, *188*(1), 657-668.

Dehghan, M., & Salehi, R. (2012). The numerical solution of the non-linear integro-differential equations based on the meshless method. *Journal of Computational and Applied Mathematics*, *236*(9), 2367-2377.

Gao, W., Veeresha, P., & Baskonus, H.M. (2023). Dynamical analysis fractional-order financial system using efficient numerical methods. *Applied Mathematics in Science and Engineering*, *31*(1), 2155152.

Gegele, O.A., Evans, O.P., & Akoh, D. (2014). Numerical solution of higher order linear Fredholm–integro–differential equations. *American Journal of Engineering Research (AJER)*, *3*(8), 243-247.

Hosseini, S.M., & Shahmorad, S. (2003). Numerical solution of a class of integro-differential equations by the Tau method with an error estimation. *Applied Mathematics and Computation*, *136*(2-3), 559-570.

Kajani, M.T., Ghasemi, M., & Babolian, E. (2006). Numerical solution of linear integro-differential equation by using sine–cosine wavelets. *Applied Mathematics and Computation*, *180*(2), 569-574.

Khan, I., Asif, M., Amin, R., Al-Mdallal, Q., & Jarad, F. (2022). On a new method for finding numerical solutions to integro-differential equations based on Legendre multi-wavelets collocation. *Alexandria Engineering Journal*, *61*(4), 3037-3049.

Kumar, R. & Arora, S. (2022). solution of fisher Kolmogorov Petrovsky equation driven via Haar scale-3 wavelet collocation method. *International Journal of Mathematical, Engineering and Management Sciences*, *7*(5), 717-729.

Kumar, R., & Bakhtawar, S. (2022). An improved algorithm based on Haar scale 3 wavelets for the numerical solution of integro-differential equations. *Mathematics in Engineering, Science & Aerospace (MESA)*,*13*(2), 617-633.

Maleknejad, K., & Mirzaee, F. (2006). Numerical solution of integro-differential equations by using rationalized Haar functions method. *Kybernetes, 35*(10), 1735-1744.

Mittal, R.C., & Pandit, S. (2017). Sensitivity analysis of shock wave Burgers' equation via a novel algorithm based on scale-3 Haar wavelets. *International Journal of Computer Mathematics*, *95*(3), 601-625.

Rahman, M. (2007). *Integral equations and their applications*. WIT Press, Southampton, UK.

Raja, M.M., Vijayakumar, V., Shukla, A., Nisar, K.S., & Baskonus, H.M. (2022). On the approximate controllability results for fractional integrodifferential systems of order 1< r< 2 with sectorial operators. *Journal of Computational and Applied Mathematics*, *415*, 114492. https://doi.org/10.1016/j.cam.2022.114492.

Saadatmandi, A., & Dehghan, M. (2010). Numerical solution of the higher-order linear Fredholm integro-differential-difference equation with variable coefficients. *Computers & Mathematics with Applications*, *59*(8), 2996-3004.

Shang, X., & Han, D. (2010). Application of the variational iteration method for solving nth-order integro-differential equations. *Journal of Computational and Applied Mathematics*, *234*(5), 1442-1447.

Shiralashetti, S.C. (2017). *A study of wavelet theory and its applications to solve integral and integro-differential equations*. Doctoral dissertation, Karnataka University. http://hdl.handle.net/10603/220545.

Wazwaz, A.M. (2001). A reliable algorithm for solving boundary value problems for higher-order integro-differential equations. *Applied Mathematics and Computation*, *118*(2-3), 327-342.

Wazwaz, A.M. (2011). *Linear and nonlinear integral equations* (Vol. 639, pp. 35-36). Springer, Berlin.

Yalçinbaş, S., & Sezer, M. (2000). The approximate solution of high-order linear Volterra–Fredholm integro-differential equations in terms of Taylor polynomials. *Applied Mathematics and Computation*, *112*(2-3), 291-308.

Yan, L., Sabir, Z., Ilhan, E., Raja, M.A.Z., Gao, W., & Baskonus, H.M. (2023). Design of a computational Heuristic to solve the nonlinear Liénard differential model: nonlinear Liénard differential model. *Computer Modeling in Engineering and Sciences*, *136*(1), 201-221.

Yusufoğlu, E. (2009). Improved homotopy perturbation method for solving Fredholm type integro-differential equations. *Chaos, Solitons & Fractals*, *41*(1), 28-37.

Yüzbaşı, Ş., Şahin, N., & Sezer, M. (2011). Bessel polynomial solutions of high-order linear Volterra integro-differential equations. *Computers & Mathematics with Applications*, *62*(4), 1940-1956.

Zemlyanova, A.Y., & Machina, A. (2020). A new B-spline collocation method for singular integro-differential equations of higher orders. *Journal of Computational and Applied Mathematics*, *380*, 112949. https://doi.org/10.1016/j.cam.2020.112949.

Zhao, J., & Corless, R.M. (2006). Compact finite difference method for integro-differential equations. *Applied Mathematics and Computation*, *177*(1), 271-288.